

Y. Hisakura^{1*}, I. Hisamitsu¹, M. Sugihara¹, S.-I. Tanifuji², H. Hamada³

¹Konica Minolta Inc., Toyokawa-shi, Aichi, Japan

²HASL Co., Ltd., Nerima-ku, Tokyo, Japan

³Kyoto Institute of Technology, Sakyo-ku, Kyoto, Japan

Material Behavior in the Plasticizing Cylinder of an Injection Molding of the Vent Type

Thermoplastic injection molding is applied in a wide variety of products. It is known that volatile components generated when resin melts cause structural defects during the thermoplastic injection process. Not only that, the pre-injection preparation work including drying the material and maintaining the metal mold, have become standard procedures to prevent these defects, but these procedures deteriorate productivity. Vent-type injection molding involves the use of cylinders featuring a vent hole at the center of the plasticizing cylinder. Although it is a conventional molding method, there are many issues including resin leakage from a vent hole and difficulty of material replacements. These issues prevented it from widespread application. Moreover, the vent-type plasticization process has not been examined theoretically or systematically. In order to maximize and generalize functions of vent-type molding, it is necessary to clarify the flow behavior of resin in the vent cylinder. In this study, we verified the flow behavior of resin in the vent-type plasticization cylinder through experimentation and simulation. In the simulation, using the flow analysis method, the filling rate inside the screw was determined by the pressure distribution inside the screw. In the experiments, the molding condition that causes venting up was verified by changing the screw rotation rates and the supply amount of the resin, for determining the filling rate of resin inside the screw. The filling rates obtained through the simulation and the experiment are almost the same. The result suggests that this simulation is very effective for predicting the filling rate.

1 Introduction

It would not be an overstatement to characterize thermoplastic injection molding as a battle with defects caused by volatile components in the raw material pellets when they are being melted for plasticization. In recent years, demand for quality in molded products has risen sharply, and manufacturers are experimenting with various additives to improve the functions such as more flame retardant, higher strength and sliding prop-

erty. Furthermore, great progresses have been made in the development and commercialization of coupling agents for additives and the matrix resin of raw material, or compounding two polymers to create an alloy. In recent years, it has become less common to use parts molded from single resin matrix. In these types of material that contain additives, the plasticization temperature of the matrix resin differs from those of the coupling agents or alloys. That promotes faster thermolysis in one material, which in turn generates more volatility. On the other hand, injection molding has not made any significant change from the conventional systems, and the battle against the volatile components is becoming more intense, as materials become more complex and diverse.

As a possible solution to these volatile constituents, about fifty years ago, an injection molding machine with a vent hole at the center of the plasticization cylinder was developed. Due to the following two reasons, the vent-type injection molding machine was not accepted in the market. First, the volatile material and the resin itself would leak out in a condition called vent-up. Secondly, the material would adhere to the screw near the vent hole at the time of material replacement. However, a new type of vent injection molding machine that can overcome the various disadvantages of the conventional vent-type injection molding machines is gaining attention recently. With the Direct Feeding Fiber Injection Mold (DFFIM) method that involves the direct feeding of the fiber into the vent hole, the mechanical strength control of resin parts is also expected (Truckenmüller and Fritz, 1991; Uawongsuwan et al., 2015; Takematsu et al., 2015).

The evaporating capacity of the vent-type injection molding machine, especially the type that completely removes moisture contained in the material, will face further price and quality competition and become an indispensable method for injection molding. For instance, molding will no longer require material drying. When this method becomes available to all producers around the world, electricity for drying will be unnecessary, removing undue burden on the environment and other associated expenses. Furthermore, due to complete moisture removal, molding defects caused by moisture will be solved. The vent-type injection molding machine has greater merits than the conventional ones. The volatile ingredient was degassed from the vent part by the update on the surface of the resin in the vent part. In this case, it is known that the devolatilization thermal efficiency is changed by the variation of the screw speed, fill-

* Mail address: Yuuki Hisakura, Konica Minolta Inc., Honohara, Toyokawa-shi, Aichi, 442-8503, Japan
E-mail: yuuki.hisakura@konicaminolta.com

ing rate, barrel temperature, etc. (Latinen, 1962; Yang and Smith, 1996; Wang et al., 1998; 2007). However, it is not easy to find plasticization conditions under which total moisture removal could be guaranteed without occurrence of the vent-up problem including resin leakage from a vent hole. There has been no theoretical or systematic analysis of the plasticization process. In order to optimize and standardize the functionality of vent-type injection molding, it is required to clarify the flow behavior of resin in the vent cylinder.

This study attempts to obtain those conditions that cause vent-up to occur from test values, and furthermore, conduct a comparison of simulation analyses to clarify the mechanisms that lead to a vent-up.

2 Theory

The screw geometry and 2.5D FEM Hele-Shaw flow element are illustrated in Fig. 1. If the gap of cylinders is sufficiently small, the flow in the H direction could be ignored. The flow field in each element is expressed by Eqs. 1 to 3.

$$u = -S \frac{\partial p}{\partial x} + DU_{bx}, \tag{1}$$

$$v = -S \frac{\partial p}{\partial y} + DU_{by}, \tag{2}$$

$$w = -S \frac{\partial p}{\partial z}. \tag{3}$$

Here, U_{bx}^e , U_{by}^e are the relative velocity of screw rotation against the wall of the barrel. The coefficient contributing to pressure gradient flow (represented as S) and the coefficient contributing to drag flow (represented as D) were calculated as shown in Eq. 4, using the definite integral value of the viscosity in the direction of thickness of each coefficient.

$$S_e = \frac{1}{H} \left(\gamma - \frac{\beta^2}{\alpha} \right), \quad D_e = \frac{1}{H} \left(\frac{H}{2} - \frac{\beta}{\alpha} \right). \tag{4}$$

Here,

$$\alpha = \int_{-H/2}^{H/2} \frac{1}{\eta} dh, \tag{5}$$

Region	Pressure P	Pressure gradient Δp	State
1	>0	>0	Filled
2	>0	<0	Filled
3	=0	>0	Unfilled

Table 1. Criteria of pressure and pressure gradient

$$\beta = \int_{-H/2}^{H/2} \frac{h}{\eta} dh, \tag{6}$$

$$\gamma = \int_{-H/2}^{H/2} \frac{h^2}{\eta} dh. \tag{7}$$

The simultaneous equation for the pressure variable defined by the contact point β of element e was calculated as shown in Eq. 8.

$$S_{\alpha\beta}^e \rho \beta^e + Q_{\alpha}^e = C_{\alpha}^e. \tag{8}$$

Here

$$Q_{\alpha}^e = \iint_{\Gamma_e} \varphi_{\alpha} [l_x u + l_y v + l_z w] d\Gamma, \tag{9}$$

$$C_{\alpha}^e = D_e U_{bx}^e \iiint_{\Omega_e} \frac{\partial \varphi_{\alpha}}{\partial x} d\Omega + D_e U_{by}^e \iiint_{\Omega_e} \frac{\partial \varphi_{\alpha}}{\partial y} d\Omega, \tag{10}$$

$$S_{\alpha\beta}^e = S_e \iiint_{\Omega_e} \left(\frac{\partial \varphi_{\alpha}}{\partial x} \frac{\partial \varphi_{\beta}}{\partial x} + \frac{\partial \varphi_{\alpha}}{\partial y} \frac{\partial \varphi_{\beta}}{\partial y} + \frac{\partial \varphi_{\alpha}}{\partial z} \frac{\partial \varphi_{\beta}}{\partial z} \right) d\Omega. \tag{11}$$

Here, S_e and D_e are defined in the gravitational center of element e, and calculated using the Eq. 5 to 7. (U_{bx}^e , U_{by}^e) are the relative velocity of screw rotation of element e, which is placed in the gravitational center against the barrel wall. Ω_e is the volume integral filled occupied by the finite element e, Γ_e is the volume boundary area of the finite element, while (l_x , l_y , l_z) represent the normal vector of the surface boundary area and φ represents the interpolation shape function in elements α and β .

The decision whether one element is filled or partially-filled (including empty) is based on the criteria of pressure and pressure gradient according to the concept of the FAN method shown in Table 1. When the pressure is larger than 0 and the

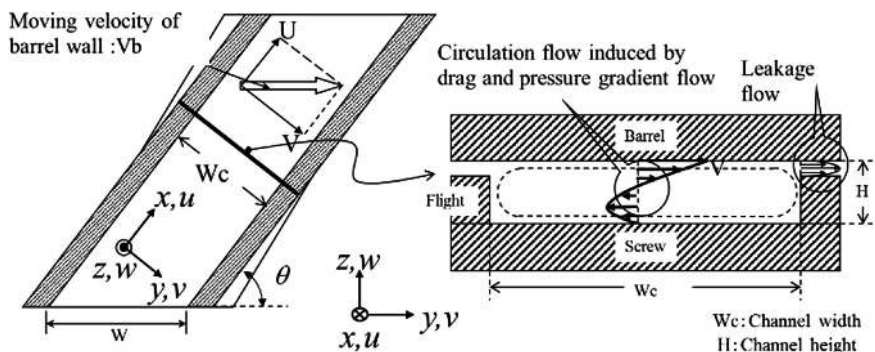


Fig. 1. Unwind modeling of the screw channel

pressure gradient is also larger than 0 (Table 1, region 1), or when the pressure is larger than 0 but the pressure gradient is smaller than 0 (Table 1, region 2) the screw is deemed to be filled with resin. When the pressure is 0 and the pressure gradient is larger than 0 ((Table 1, region 3), the screw is not filled. The average fill rate is:

$$f^{av} = \frac{Q_e}{Q_d}, \tag{12}$$

where Q_e is the filling rate of each element, Q_d is the volume of the screw groove of each element.

3 Experimental

3.1 Materials

An acrylonitrile butadiene styrene (ABS: grade Cevian SF500) polymer was used as the matrix. ABS was supplied by Daicel Polymer Ltd., Tokyo, Japan.

3.2 Sample Preparation

The structure of the actual vent-type injection mold machine used for the experiments is shown in Fig. 2. The injection molding machine (J110AD, JWS, Tokyo, Japan) has the clamping force of 110 tons, but two barrels were used for the experiments; one was a normal ventless barrel, the other one was vented and manufactured by Nihon Yuki, Sagamihara, Japan. The screw diameter was 35 mm for the normal barrel, 30 mm for the vented barrel. The vent-type has a vent hole at the center of the plasticization cylinder that releases gases and moisture generated by the resin. It is also equipped with a feeder that sup-

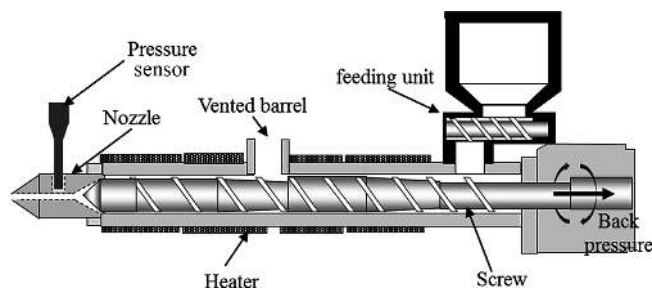


Fig. 2. Schematic of the injection molding process

plies material with constant quantities. The diameter around the nozzle was prepared in two sizes, $\phi = 3$ mm and $\phi = 6$ mm, and these nozzles were used for both the ventless and vented barrels. A pressure sensor (NP463, Dynisco, Franklin, MA, USA) was attached to the nozzle to measure the amount of pressure created by the plasticized resin. For this experiment, the resin volume supplied from the feeder and screw rotation were set as parameters. The barrel temperature was 240°C, the back pressure was set at the highest value possible for molding machines as 45 MPa, the screw was rotated without retreat and calculated the amount of resin that was discharged. The discharge volume was calculated as g/sec and measured in seconds. After confirming venting or non-venting action, the back pressure and nozzle pressure at the time of discharge were calibrated. The filling rate was calculated after the discharge amount was measured, then the screw was removed and the volume was measured at each L/D interval.

Figure 3 shows the structure of the screw used for vent-type molding and normal-type molding. Table 2 shows the parameters of the normal molding and vent-type molding screws. The normal screw measures 35 mm in diameter and 1.8 in compression ratio. The vent-type screw measures 30 mm in diameter, with the compression ratio at 1.8 at stage 1 and 1.6 at the stage (from the hopper to the nozzle, the pre-vent phase is referred to as stage 1, and the post-vent phase as stage 2).

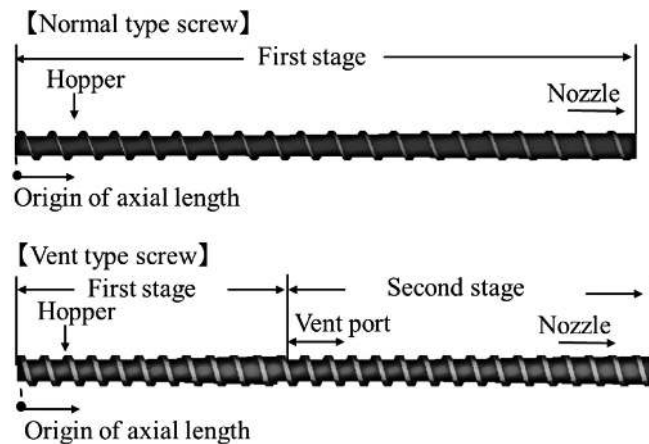


Fig. 3. Structure of vent molding screw

	Screw length mm	First stage		Second stage	
		Compression rate	Screw length mm	Compression rate	Screw length mm
Normal screw	700	1.8	700	–	–
Vent screw	780	1.8	510	1.6	270

Table 2. The parameters of the normal molding and vent-type molding screws

4 Results and Discussion

4.1 Results of Vent-Up Testing

Table 3 shows the results of the tests conducted on a normal barrel and a vented barrel. The pressure value at the nozzle and the resin discharge amount per 60 s or 1 s were recorded at each screw rotation and feeder rotation, respectively. In the case of the vented barrel, the venting-up volume was also recorded in the 60 s interval.

Figure 4 shows the relationship between screw speed and nozzle pressure. When the feeder speed is fixed, there is very

little difference in the discharge amount for both normal and vented barrels. Furthermore, no pressure increase was detected at the nozzle for the normal barrel and vented barrel with the $\phi = 6$ mm diameter. However, for the vented barrel with the $\phi = 3$ mm diameter, the nozzle pressure rises as the rotation number of the screw decreases. When the pressure reached 13 MPa, equivalent to a screw speed of 30 min^{-1} , venting-up occurred. This is because a higher rotation count of the feeder induced an increase in flow. Figure 5 shows the relationship between the rotation speed of the feeder and nozzle pressure. As the rotation number of the feeder increases, resin supply amount also increases. It brings an increase in the resin

No	Screw speed min^{-1}	Feeder speed min^{-1}	Normal barrel Nozzle diameter: $\Phi 6$		
			Pressure at nozzle MPa	Discharge amount g/60 s	Discharge amount g/s
1	30	70	5.57	63.7	1.01
2	65	70	5.32	61.7	0.98
3	135	70	5.37	60.4	0.96
4	170	70	5.32	64.9	1.03
5	205	70	5.52	63.8	1.01
6	100	30	3.86	23.0	0.36
7	100	50	5.67	40.1	0.64
8	100	70	5.72	60.8	0.97
9	100	90	7.17	81.3	1.29
10	100	110	7.72	99.5	1.58
11	100	130	8.68	116.6	1.85
12	100	150	10.03	142.4	2.26

A)

Table 3. (Continued)

No	Screw speed min^{-1}	Feeder speed min^{-1}	Vent barrel Nozzle diameter: $\Phi 3$			
			Pressure at nozzle MPa	Discharge amount g/60 s	Vent-up amount g/60 s	Discharge amount g/s
1	30	70	13.06	65.0	24.6	1.42
2	65	70	12.57	63.4	–	0.98
3	135	70	10.17	59.5	–	0.99
4	170	70	9.15	60.8	–	0.99
5	205	70	8.13	63.1	–	0.98
6	100	30	7.94	26.8	–	0.41
7	100	50	9.51	43.4	–	0.69
8	100	70	11.34	61.7	–	0.97
9	100	90	10.86	75.6	–	1.24
10	100	110	11.61	93.7	–	1.51
11	100	130	12.63	114.7	5.4	1.95
12	100	150	13.90	133.4	13.6	2.32

B)

Table 3. (Continued)

No	Screw speed min ⁻¹	Feeder speed min ⁻¹	Vent barrel Nozzle diameter: Φ6			
			Pressure at nozzle MPa	Discharge amount g/60 s	Vent-up amount g/60 s	Discharge amount g/s
1	30	70	5.7	53.4	—	0.85
2	65	70	5.2	57.8	—	0.92
3	135	70	5.7	58.3	—	0.93
4	170	70	5.2	60.7	—	0.96
5	205	70	4.9	57.7	—	0.92
6	100	30	4.7	28.1	—	0.45
7	100	50	5.1	45.1	—	0.72
8	100	70	5.2	56.6	—	0.90
9	100	90	5.2	74.9	—	1.19
10	100	110	5.8	90.4	—	1.44
11	100	130	6.3	107.2	—	1.70
12	100	150	7.3	124.5	—	1.98

C)

Table 3. Test results on normal barrel and vented barrel, A) results for normal barrel/ $\phi = 6$ mm diameter nozzle, B) results for vented barrel/ $\phi = 3$ mm diameter nozzle, C) results for normal barrel/ $\phi = 6$ mm diameter nozzle

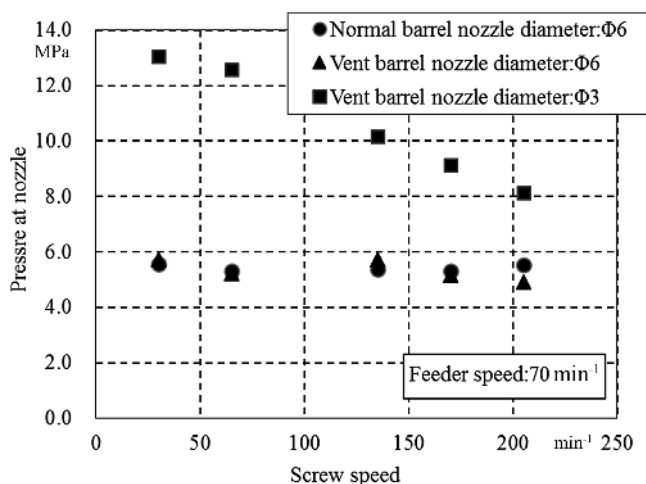


Fig. 4. Relationship between screw rotation rate and nozzle pressure

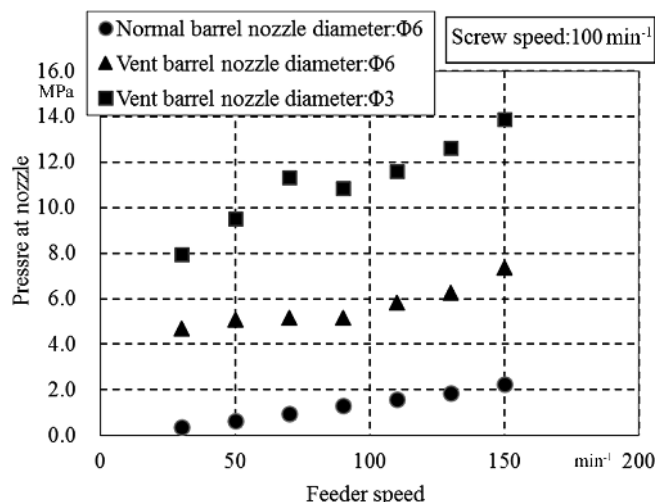


Fig. 5. Relationship between feeder rotation rate and nozzle pressure

discharge amount. It can be observed that this leads to an increase in nozzle pressure for both normal and vented barrels. Nozzle pressure rises considerably from a normal cylinder/vented barrel with the $\phi = 6$ mm diameter nozzle to a vented barrel with the $\phi = 3$ mm diameter nozzle. Venting-up occurred from around 12.6 MPa.

4.2 Comparative Analysis of Test Results

Based on theory, we calculated the pressure in the axial direction and filling rate, using the discharge amounts obtained from

test results and the nozzle tip pressure as input values. Figure 6 shows the relationship between the screw speed of the normal barrel, and the pressure toward the shaft and the screw speed. The numbers in the legend correspond to the experiment number. In conjunction with the drop in screw speed, it was observed that the pressure slope toward the screw shaft from the nozzle tip to the hopper decreased. When decreasing the screw speed while keeping the flow volume constant, the transport volume of the screw material decreases, which increases the filling rate. Therefore, the decrease in speed results in pressure increases.

Figure 7 shows the relationship between the feeder rotation speed, pressure in the axial direction and the screw speed. The

numbers in the legend correspond to the experiment number. Test results indicate that an increase in the rotation speed of the feeder, or the resin flow volume, boosts pressure on the nozzle tip. And an increase in the nozzle tip pressure increases the pressure in the direction of the hopper, but because the screw speed remains constant, the pressure shift remains steady.

Figure 8 shows the relationship between the screw rotation speed for a vent barrel/nozzle with the $\phi = 3$ mm diameter, pressure toward the shaft, and screw speed. Figure 8A shows the axial direction pressure from the vent hole to the nozzle, and Fig. 8B shows the close-up of the area around the vent hole. There is a vent hole with 480 to 550 mm on the barrel. The structure of the screw on the vent barrel is divided into two stages, stage 1 and stage 2. Compression is applied in two places, the part in front of the vent and at the nozzle. Therefore, it can be observed that there is pressure at the compression spot in front of the vent, although at a much smaller value compared

with the nozzle pressure. With regards to pressure in the nozzle area, the pressure impact on the screw speed is the same as on the normal barrel, and the pressure shift toward the screw shaft decreases in line with a decrease in the screw speed. However, compared with the normal barrel, the vent barrel/nozzle with the $\phi = 3$ mm diameter has a higher pressure value at the nozzle tip according to test results: a pressure increase to about 650 mm was measured. Under condition (1) at 30 min^{-1} , it was observed that venting-up has occurred, with a rise in pressure on the nozzle tip caused the venting-up. Figure 9 shows the relationship between the feeder rotation speed of the vent barrel/nozzle with the $\phi = 3$ mm diameter, pressure in the axial direction and the screw rotation speed. Figure 9A shows the axial direction pressure from the vent hole to the nozzle, and Fig. 9B shows the close-up of the area around the vent hole. Even if increasing the flow volume did not exert much influence on the pressure of the compressed area before the vent hole, as compared with the pressure against the nozzle tip.

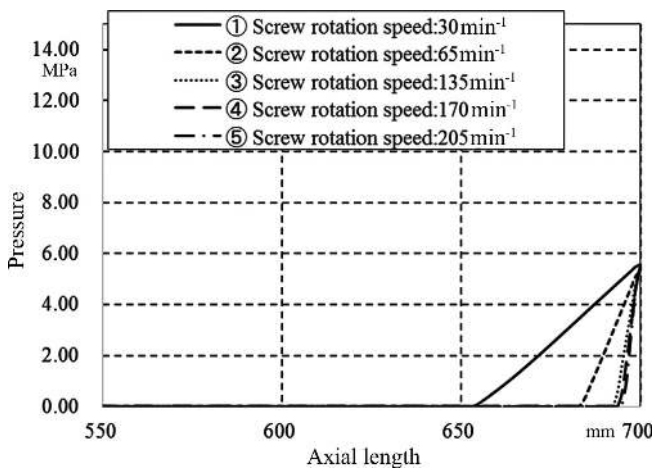


Fig. 6. Relationship between screw rotation rate for normal barrels, pressure in the axial direction and screw rotation numbers

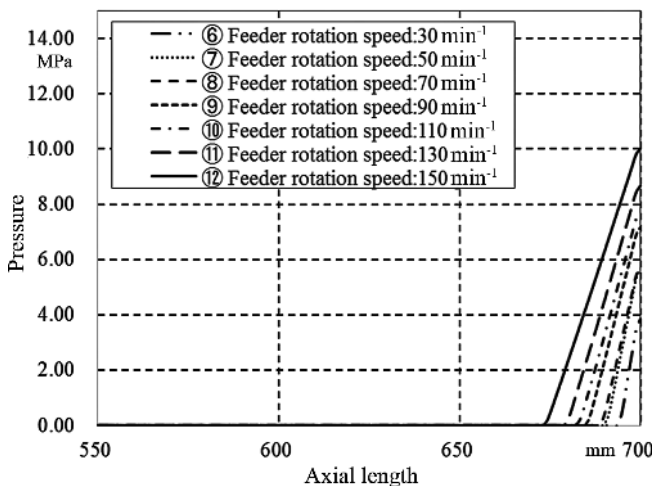
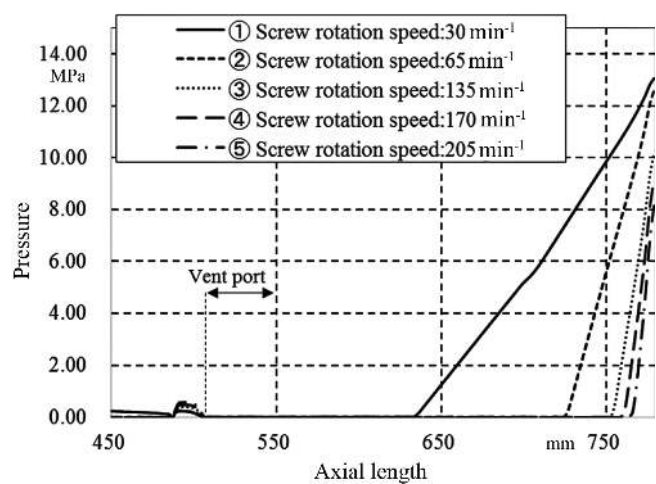
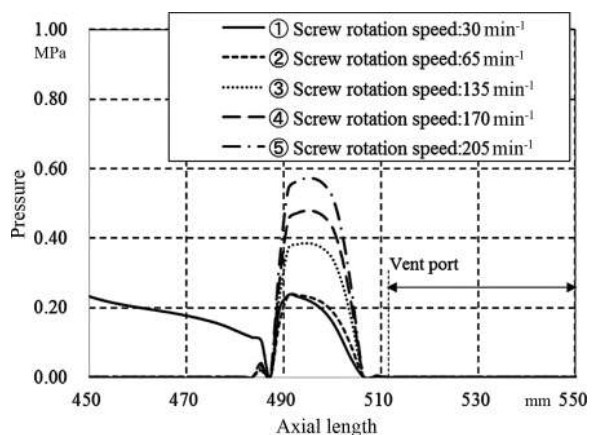


Fig. 7. Relationship between feeder rotation rate for normal barrels, pressure in the axial direction and screw rotation numbers



A)



B)

Fig. 8. Relationship between for vent barrel/nozzle with the $\phi = 3$ mm diameter, pressure in the axial direction and screw rotation speed, A) axial direction pressure from the vent hole to the nozzle, B) the close-up of the area around the vent hole

Pressure in the nozzle area has the same tendency as the pressure shift in the normal barrel, without changes in the pressure shift caused by changes in flow. However, comparing the vent with a $\phi = 3$ mm barrel with a normal barrel, as the test results show a higher pressure value on the nozzle tip, a pressure increase to around 740 mm was confirmed. Venting-up was generated in conditions (11) and (12), caused by a rise in pressure at the nozzle tip.

Figure 10 shows the relationship between the screw speed and axial direction pressure for vent barrel/nozzle with the $\phi = 6$ mm diameter, and the screw rotation numbers. Figure 11 shows the relationship between the feeder speed for vent barrel/nozzle with the $\phi = 6$ mm diameter and the axial direction pressure, and the screw speed. Figure 11A shows the axial direction pressure from the vent hole to the nozzle, and Fig. 11B shows the close-up of the area around the vent hole. Test results show that the pressure value is smaller than that of vent barrel/nozzle with the $\phi = 3$ mm diameter, but showing similar tendencies.

Venting-up did not occur for vent barrel/nozzle with the $\phi = 6$ mm diameter under either condition. Because the pressure on the nozzle tip is small, it suggests that it caused the small pressure increase from the nozzle toward the hopper. Comparing pressure increases under condition (1) at 30 min^{-1} , vent barrel/nozzle with the $\phi = 3$ mm diameter shows an increase at around 640 mm, while $\phi = 3$ mm showed an increase at around 740 mm. It suggests that venting-up is closely related to pressure conditions around the nozzle.

Figure 12 shows the results of a filling rate at a screw rotation rate of 30 min^{-1} and a feeder rotation rate of 70 min^{-1} on a normal barrel. Test values were obtained by calculating the resin volume at every interval after the screws were removed at the end of testing. Both test and calculated values show the increase in filling rates toward the nozzle, indicating a correlation. However, the filling rate of the test value shows the tendency to increase in the area of 400 to 500 mm against the calculated value. Over 500 mm to 600 mm, the test value tends to

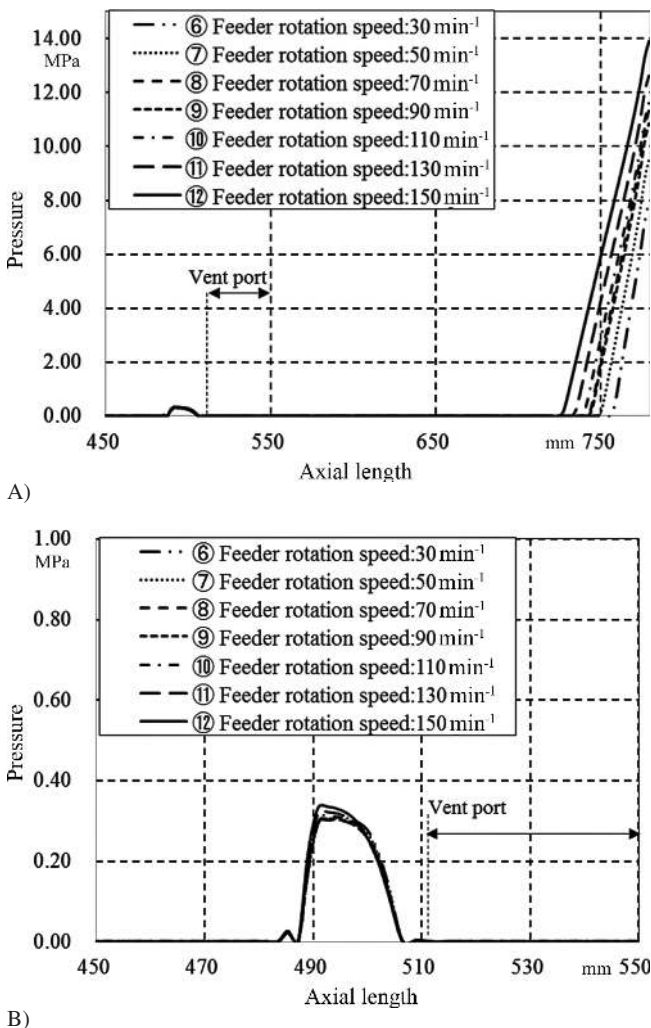


Fig. 9. Relationship between feeder rotation rate for vent barrel/nozzle with the $\phi = 3$ mm diameter, pressure in the axial direction and screw rotation numbers, A) axial direction pressure from the vent hole to the nozzle, B) the close-up of the area around the vent hole

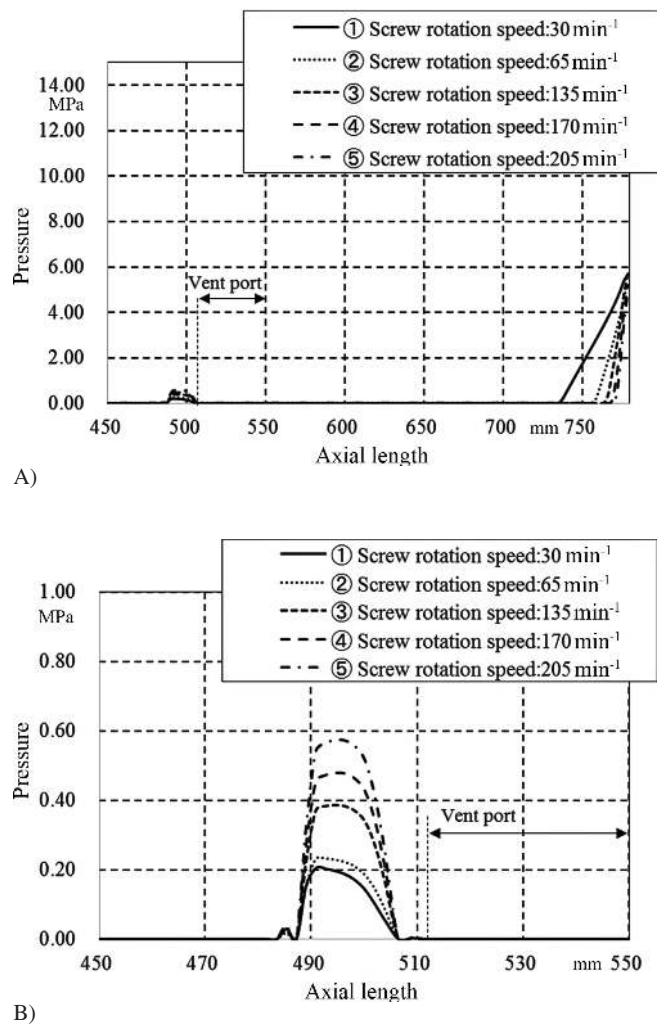


Fig. 10. Relationship between screw rotation rate for vent barrel/nozzle with the $\phi = 6$ mm diameter, pressure in the axial direction and screw rotation speed, A) axial direction pressure from the vent hole to the nozzle, B) the close-up of the area around the vent hole

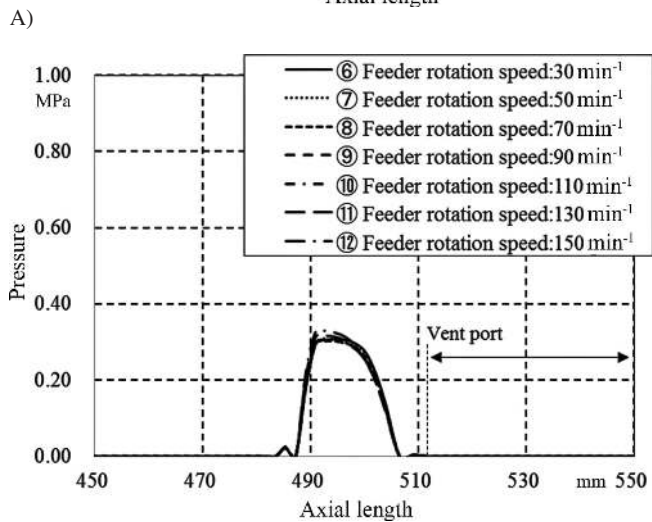
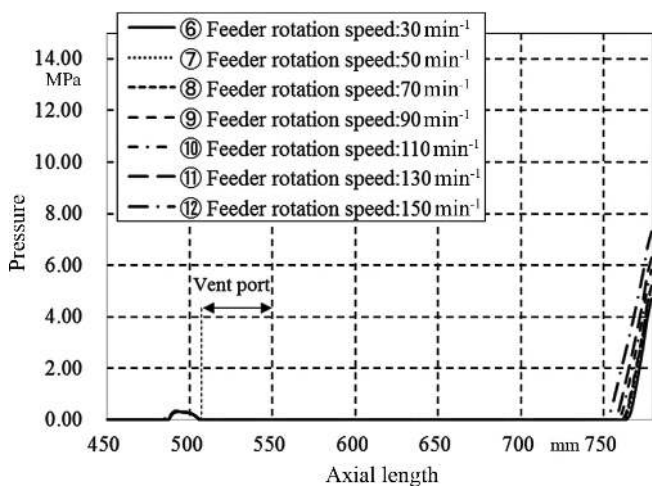


Fig. 11. Relationship between screw rotation rate for vent barrel/nozzle with the $\phi = 6$ mm diameter, pressure in the axial direction and screw rotation speed, A) axial direction pressure from the vent hole to the nozzle, B) the close-up of the area around the vent hole

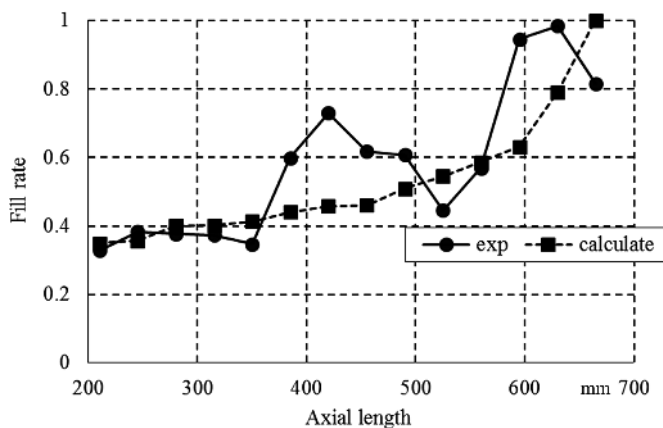


Fig. 12. Filling rate of normal barrel: screw rotation rate of 30 min^{-1} and feeder rotation rate of 70 min^{-1}

be lower in the filling rate compared to the calculated value. Figure 13 shows a photo of removing a screw and simulated filling rate for the normal barrel: screw rotation rate of 30 min^{-1} , feeder rotation rate of 70 min^{-1} . Fig. 13B is a contour map of the calculated results of the filling rate. The part indicated by the arrow at the center in the screw axis direction of the photo is the place where the filling rate increased. When the supply amount of resin was lower than the drag flow rate of the screw, or in the starved state, pressure was not generated inside the cylinder. Therefore, it can be inferred that the resin stagnated because the friction between the resin and the inside of the cylinder decreased, which triggered the decrease of the filling rate. The calculation does not account for any resin stagnation and therefore causing an error in the filling rate. It is believed that there was not enough material to be drawn out toward the nozzle and it stagnated.

Figure 14 shows the results of the filling rate for the vented barrel/ ϕ diameter nozzle with a 30 min^{-1} screw rotation rate, and a 70 min^{-1} feeder rotation rate. Figure 15 compares a photo of removing a screw with the simulated filling rate for a vented barrel: screw rotation rate of 30 min^{-1} and feeder rotation rate

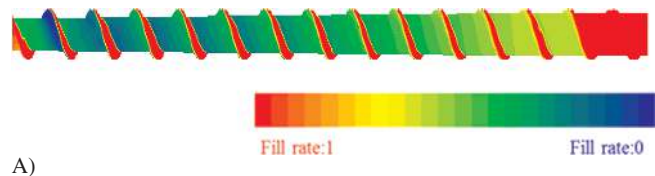


Fig. 13. Comparison of a photo of removing a screw and the simulated filling rate of a normal barrel: screw rotation rate of 30 min^{-1} , feeder rotation rate of 70 min^{-1} , A) simulated filling rate (red indicates a full barrel, blue indicates a partially full barrel), B) picture of removing a screw

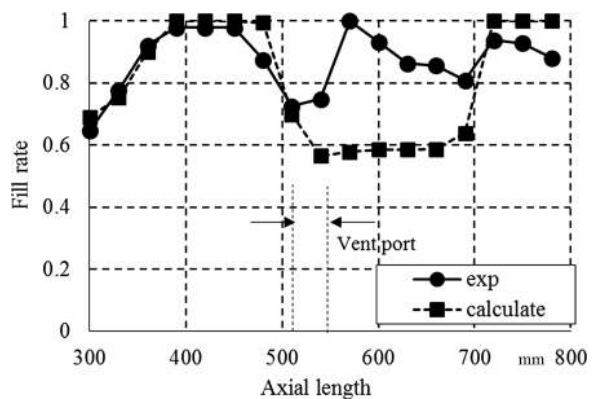


Fig. 14. Filling rate of vented barrel/ $\phi = 3$ mm diameter nozzle: screw rotation rate of 30 min^{-1} and feeder rotation rate of 70 min^{-1}

of 70 min^{-1} . The vent type screw has the structure in which the front of the vent port is the first stage and the back of the vent port is the second stage. These conditions indicate the occurrence of venting-up. The vent hole exists in the rear between 480 to 550 mm. Compared with the normal barrel, the filling rate rises for the vented barrel at the stage 1 compression area and stage 2 compression area. During stage 1 from the vent hole to the hopper, the test value is nearly identical to the calculated value with matching tendency.

In stage 2, from the vent hole to the nozzle side, the filling rates are more likely to increase toward the nozzle in both the test value and the calculated value, and they are almost consistent. However, the test values show a slightly higher filling rate toward the vent hole, but a slightly lower toward the nozzle, compared to the calculated value. This suggests that the higher pressure toward the nozzle and the lower filling rate around the vent hole weakened the resin supply force, which eventually induced the resin stagnation. Therefore, even if the calculation rates show no resin filling rate around the vent hole, venting-up still occurs due to the stagnation of the resin. Figure 16 shows the results of the filling rate for the vented barrel/nozzle with the $\phi = 3 \text{ mm}$ diameter at 205 min^{-1} screw rotation rate and a 70 min^{-1} feeder rotation rate. Figure 17 shows a comparison of a photo of removing a screw with the simulated filling rate from a vented barrel: screw rotation rate of 30 min^{-1} and feeder rotation rate of 70 min^{-1} . These conditions indicate the occurrence of venting-up. According to the calculated results, the filling rate doesn't reach 1 in the direction of the shaft in either place. Compared with the screw rotation rate of 30 min^{-1} , the error from the test value is widening. It can be inferred that there is no place where the filling rate reaches 1, which is caused by resin stagnation in all places. Figures 14 to 17 show the influence of filling rate due to screw rotation. It is shown that vent up occurred at low screw speeds. Similarly, in the case of the feeder rotation, when the feeder rotation speed is high,

it is assumed that the filling rate in the screw increases and vent-up occurred.

Due to the above results, it is necessary to calculate and find a place between the vent hole and the nozzle that can achieve a filling rate of 1, then predict that distance. We can predict as shown in the test results in Fig. 14 that somewhere between post-venting and up to around 750 mm of resin pressure, venting-up will occur. When checking with filling rate, if there is any section, between 700 mm and the nozzle tip, where the calculated value of the filling rate reaches 1, the occurrence of venting up can be predicted. Either lowering the feeder rotation rate or lowering the screw rotation rate was found to be effective to prevent venting up. Through this method, the filling rate of resin inside the screw decreases, which forms the ideal molding condition where venting up is unlikely to occur.

Furthermore, there is measuring process in actual molding work and the positional relationship changes where the vent

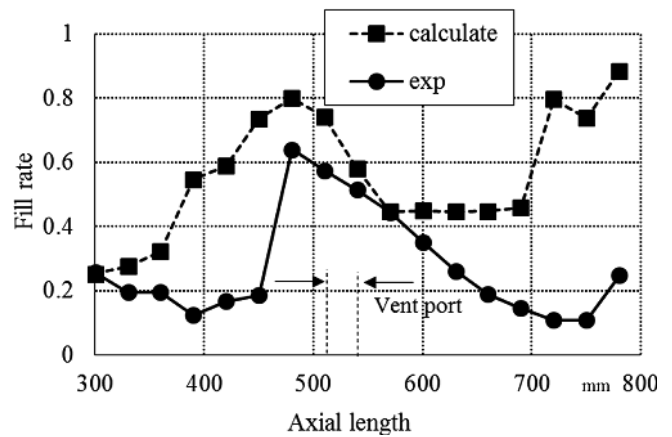


Fig. 16. Filling rate of a vented barrel screw: screw rotation rate of 205 min^{-1} and feeder rotation rate of 70 min^{-1}

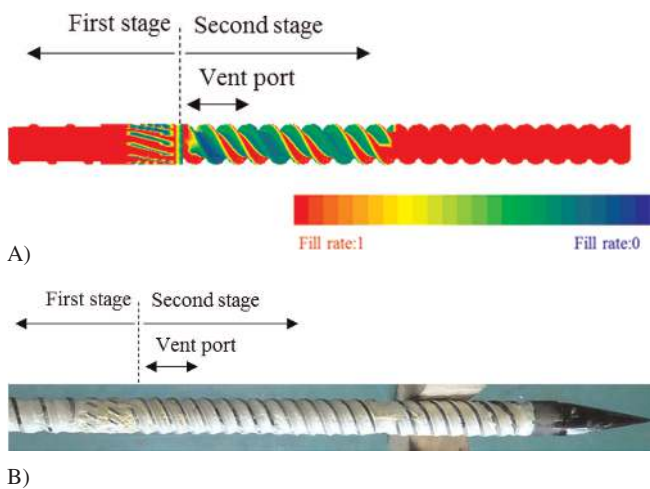


Fig. 15. Comparison of a photo of removing a screw and simulated filling rate from a vented barrel: screw rotation rate of 30 min^{-1} and feeder rotation rate of 70 min^{-1} , A) simulated filling rate (red indicates a full barrel, blue indicates a partially full barrel), B) picture of removing a screw

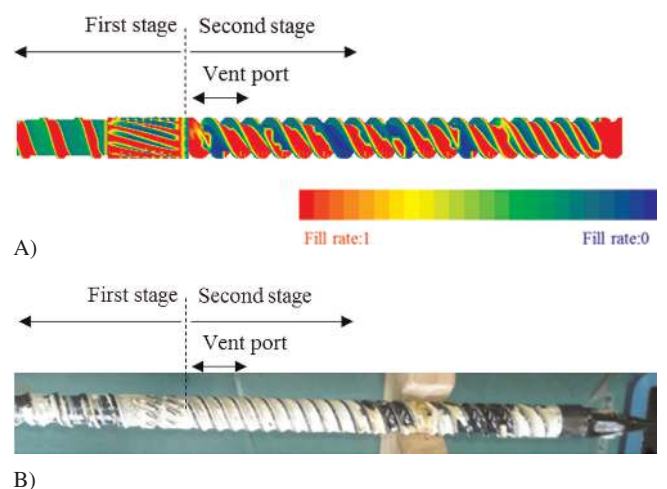


Fig. 17. Comparison of a photo of removing a screw and simulated filling rate from a vented barrel: screw rotation rate of 205 min^{-1} and feeder rotation rate of 70 min^{-1} , A) simulated filling rate (red indicates a full barrel, blue indicates a partially full barrel), B) picture of removing a screw

and the filling rate become 1, thereby variables must be taken into consideration when predicting venting-up.

5 Conclusion

The venting-up mechanism of a vent-type injection molding machine is, when the pressure on the nozzle side rises, the resin filling rate near the nozzle increases. In other words, the increase of pressure on the nozzle side is one of the main factors to induce venting-up. The rotation speed of the screw is a major factor that increases the resin pressure between the vent hole and the nozzle. Reducing the screw rotation rate lowers the amount of material delivered, and that eventually raises the filling rate. Upon comparing experimental and calculated values of filling rates, we can predict the occurrence of venting-up by comprehending the screw position that brings filling rates to 1. However, resin stagnation can cause calculation errors. For this molding machine, if having a screw length of 780 mm with a hopper side at a 0 mm standard, venting-up potentially occurs when the filling rate becomes 1 or less with the pressure in the nozzle side below 750 mm. As for the resin stagnation, the difference between the actual flow volume and the possible drag flow of the screw becomes wider; it is more likely an error will occur. These shall be considered in a future discussion concerning filling rate calculations.

References

Latinen, G. A., "Devolatilization of Viscous Polymer Systems", *Adv. Chem. Series*, **34**, 235–246 (1962)

- Takematsu, R., Uawongsuwan, P., Inoya, H. and Hamada, H., "Direct Fiber Feeding Injection Molding of Glass Fiber Reinforced Polycarbonate/ABS Polymer Blends Composites", *SPE ANTEC Tech. Papers*, 451–456 (2015)
- Truckenmüller, F., Fritz, H.-G., "Injection Molding of Long Fiber-Reinforced Thermoplastics: A Comparison of Extruded and Pultruded Materials with Direct Addition of Roving Strands", *Polym. Eng. Sci.*, **31**, 1316–1329 (1991), DOI:10.1002/pen.760311806
- Uawongsuwan, P., Okoshi, M., Inoya, H. and Hamada, H., "Modification of Interfacial Bonding of Hybrid Glass Fiber/Carbon Fiber Polypropylene Composite Fabricated by Direct Fiber Feeding Injection Molding", *SPE ANTEC Tech. Papers*, 577–582 (2015)
- Wang, N. H., Hashimoto, N. and Sakai, T., "An Experimental Study on Devolatilizing Performance on a Long Vent Section in a Twin Screw Extruder", *Seikei Kakou*, **11**, 755–760 (1994)
- Tomiyama, H., Takamoto, S., Shintani, H. and Inoue, S., "Devolatilization Analysis in a Twin Screw Extruder by Using the Flow Analysis Network (FAN) Method", *Seikei Kakou*, **9**, 565–574 (2007)

Date received: August 17, 2017

Date accepted: December 30, 2017

Bibliography
 DOI 10.3139/217.3572
 Intern. Polymer Processing
 XXXIII (2018) 5; page 652–661
 © Carl Hanser Verlag GmbH & Co. KG
 ISSN 0930-777X